Article

JOURNAL OF REINFORCED PLASTICS & COMPOSITES

Journal of Reinforced Plastics and Composites
30(18) 1539–1547

DOI: 10.1177/0731684411421844
jrp.sagepub.com

SAGE

Mechanical and energy absorption behaviors of metal/polymer layered sandwich structures

S. Bahar Başẗurk and Metin Tanoğlu

Abstract

This article considers the sandwich structures with aluminium (Al) foams of various thicknesses in conjunction with skins composed of fibre-metal laminates (FML). The FMLs with Al sheet and glass fiber reinforced polypropylene (GFPP) composites were integrated with Al foam for composing the sandwich panels. The FML–foam sandwich systems were manufactured by hot pressing in a mold at 200°C under 1.5 MPa pressure. The bonding between the components of the sandwich was achieved by various surface modification techniques, i.e., silane surface treatment, PP adhesive film addition, and their combination. The Al sheet/Al foam sandwiches were also prepared by bonding the components with an epoxy adhesive for comparing the effect of GFPP on the mechanical performance of the sandwich structures. The energy absorption capacities together with compressive mechanical behavior of both Al foams and FML-foam sandwich systems were evaluated by flatwise compression tests. Experiments were performed on samples of varying foam thicknesses.

Keywords

fiber/metal laminates, Al foam, sandwich composites, interface, mechanical behavior

Introduction

Due to the light weight and energy absorption capabilities, fiber–metal laminates (FMLs) consisting of thermoplastic composite layers offer great potential in many applications such as aerospace, automotive, transportation industry, and anti-blast armor systems.[1] Metallic foams have some potential to be used in different engineering applications due to their high specific stiffness and strength, fire resistance, noise reduction, vibration damping, and cost efficiency.[2] Besides all these superior properties, the energy absorption capability of the aluminum (Al) foams against dynamic loads makes them useful specifically in impact-related applications. Various production techniques with different chemical compositions greatly affect the microstructural and mechanical properties of foams. A great number of studies[3–10] are available in the literature which contains conventional tests applied to the Al foams to reveal their mechanical performances under different loading conditions. Particularly, the quasi-static compressive responses of Al foams were investigated by a number of researchers and it was found that the stress–strain graphs of foams show a significant characteristic with three distinct regions. The first region with linear elasticity corresponds to small deformation by the bending of cell edges and stretching of cell walls. In the second region, a long plateau part is present with almost the constant stress value. This zone has vital importance for the applications requiring energy absorption capability. The last region is called as 'densification' where the cell walls are in close contact and a steep stress increase is observed.[3–6] McCullough et al.[7] investigated the tensile and compressive characteristics of closed-cell ALULIGTH^{TM} Al foams by considering their deformation mechanisms. The foams exhibited semi-brittle behavior

Department of Mechanical Engineering, İzmir Institute of Technology, Gulbahçe Koyu, Turkey.

Corresponding author:
Metin Tanoğlu, Department of Mechanical Engineering, İzmir Institute of Technology, Gulbahçe Koyu, 35430, Urla, İzmir, Turkey
Email: metintanoglu@iyte.edu.tr

under tension while they showed ductility under compression due to the different failure modes. Motz and Pippan[8] reported a study about the tensile properties of ALPORAS™ Al foams with different densities. It was observed that the stress–strain curves of foams under tension exhibited dissimilarities compared to the compression. The linear elastic regime is followed by a plastic regime with the formation of fracture process zone and the crack progression led to the failure of Al foam. The strain at fracture was rather small under tensile loading and the foams with higher density showed relatively higher failure strains. Deqing et al.[9] reported the compressive properties of Al foams by considering their cell structures. In their study, it was found that both plastic collapse strength and energy absorption capacities of the closed-cell aluminum foams were significantly improved by decreasing the cell size of the foams having the same density. Koza et al.[10] concentrated on the compression behaviors of Al foams having various densities and dimensions. Based on their studies, larger samples showed lower mean strength and narrower scattering of the strength values than those of the smaller ones. This behavior was described in terms of a greater probability of the presence of lower density parts in the former foam samples. Bastawros et al.[11] focused on the plastic deformation progression of Al foams under compressive loading using digital image correlation procedure. The strain maps were monitored and the deformation patterns of the foams obtained with this technique.

Sandwich panels containing metallic foams with minimal weights, desired stiffness, and strength can be designed for numerous applications. The optimization of design parameters, such as material types of core, face sheets, and design geometry of the panel, has great importance with the knowledge of dominant failure mechanism at critical loads. Researchers have generally focused on flexural and buckling behaviors of aluminum foam sandwiches under static or dynamic loading.[12] McCormack et al.[13] investigated the failure characteristics of metal foam sandwich structures using aluminum metal skins. Styles et al.[14] concentrated on aluminum foam sandwiches with composite skins. The flexural behavior of sandwiches under three- or four-point bending test was characterized in order to identify the failure modes produced by altering core thickness and span length. The sandwiches were found to fail generally by core shear, indentation, face-sheet yielding, or wrinkling.[15]

A unique type of materials called FMLs have been developed as armor systems against blast and ballistic effects, due to their high energy absorption characteristics. In the generation of FMLs, instead of thermoset plastics, the fiber-reinforced thermoplastic composites offer better solutions due to their higher energy absorption behavior, toughness, and process flexibility. The sandwich panels manufactured based on thermoplastic FML skins and an aluminum foam core were considered as an alternative configuration for the blast applications[14,15]. Langdon and Cantwell[2] reported the applications of aluminum foam sandwiches with FMLs. Several dynamic tests were carried out in order to evaluate the performance of these sandwiches under low- and high-velocity impacts. The combination of thermoplastic-based composite face-sheets with aluminum plate and aluminum foam led to the increase of energy absorption capability. It was also found that the use of FML systems provides significant improvement in terms of ballistic protection and damage resistance.[16] Reyes[17] studied the flexural and low-velocity impact behaviors of the FML-reinforced sandwich panels with aluminum foam core. It was found that the failure mechanisms of the sandwich components contributed to the energy absorption capability of the system and the proposed energy balance model was in good agreement with the experimental results. Tanoğlu et al.[18] investigated the compression and energy absorption characteristics of Al foams and Al foam-based sandwiches bonded with epoxy and silane surface treatments. They found that the foams with higher elastic modulus showed generally higher collapse strength for each thickness set of foams and foam-based sandwiches. The foam thickness increase resulted in the increase of elastic modulus for the as-received Al foams. The thickness increase generally leads to increase of energy absorption capacity and the Al sheet/GFPP/Al (GFPP, glass fiber reinforced polypropylene) foam sandwiches showed maximum absorbed energy (AE) values due to the contribution of GFPP.

In this study, sandwich structures containing FML face-sheets and core material were developed by integrating the Al foam, Al sheet, and GFPP composites with the addition of polypropylene (PP)-based adhesive film application with or without silane surface treatment. The flatwise compression properties of both as-received foams and foam-based sandwiches with various foam thicknesses (8, 20, and 30 mm) were investigated under quasi-static loading conditions. Also, the sandwich systems composed of Al sheet/Al foam bonded with epoxy were produced in order to compare the effect of GFPP in terms of mechanical performance. The energy absorption capabilities of the foams and foam-based sandwiches were also characterized.

Materials and test procedure

Aluminum sheets and aluminum foams with various thicknesses were used to produce the sandwich structures used in this study. The physical and geometrical properties

of the materials used in the experiments are tabulated in Table 1. The closed-cell aluminum foam material (supplied by Shinko Wire Company Ltd., Austria) with the trade name ALULIGHT-AFS® was employed as a core material. The Al foam specimens were cut from the large panels with thicknesses 8, 20, and 30 mm, as shown in Figure 1. The foam panels were covered on both surfaces with a skin of about 0.6 mm thick and strongly bonded, produced during the manufacture of the foam. The 2 mm thick Al sheets were attached onto the top and bottom surfaces of the foams as face-sheets to prepare sandwiches. In this study, the sandwich components were bonded together after some surface modification techniques and/or adhesive film application. The adhesives, sandwich configurations, and their processing techniques are listed in Table 2. The as-received (monolithic) Al foams and the sandwiches prepared with those foams are illustrated in Figure 1.

A commercial epoxy adhesive (Bison®) was applied between the Al face-sheet and Al foam in order to obtain Al sheet/Al foam sandwiches (AFS, Al foam based sandwiches). The woven cloths consisting of comingled glass and polypropylene fibers with a glass fiber volume fraction of 60% (Telateks® Inc, Turkey) were stuck between Al sheet and Al foam as an intermediate layer for producing hybrid Al sheet/GFPP/AL foam (AFS) sandwich structure. structure. Dow-Corning® Z-6032 silane was also used for providing robust bonding between GFPP-Al sheet and GFPP-Al foam interfaces. For the surface modification with silane coupling agent, Al sheet and Al foam surfaces were first degreased, and then modified with silanes based on the procedure reported by the manufacturer.[19] Sandwich structures with modified PP adhesive layers were also developed. For this purpose, 20 wt% maleic anhydride modified polypropylene (PP–g–MA) and PP blends were prepared using twin screw extruder (EUROLAB®). The blend was formed as fine granules, as shown in Figure 2(a). The cooled blend was pressed at 185°C under the fixed pressure of 1 MPa by hot pressing to obtain PP–g–MA-based adhesive films with 0.5 mm thickness, as shown in Figure 2(b). PP–g–MA layer was incorporated at the Al–GFPP interface during the preparation of the sandwich structures. The combined effect of silane surface modification and PP–g–MA-based adhesive film application on the same sandwich samples was also investigated in this study. The Al sheet and Al foam surfaces were first treated with silane and then PP-based films were introduced at the interface of the components of sandwiches during sandwich fabrication.

The flatwise compression tests were applied to the samples in order to characterize the compression behavior of as-received Al foams and Al foam based

Table 1. Physical and geometrical properties of materials used to prepare sandwich composites

Material	Average thickness (mm) (± standard deviation)	Average density (g/cm$^{3)}$ (± standard deviation)
Al foam	7.8 (0.1)	0.409 (0.006)
	18.95 (0.1)	0.395 (0.003)
	29.9 (0.1)	0.456 (0.007)
GFPP	0.65 (0.2)	1.254 (0.04)
Al sheet	2.01 (0.2)	2.7 (0.01)

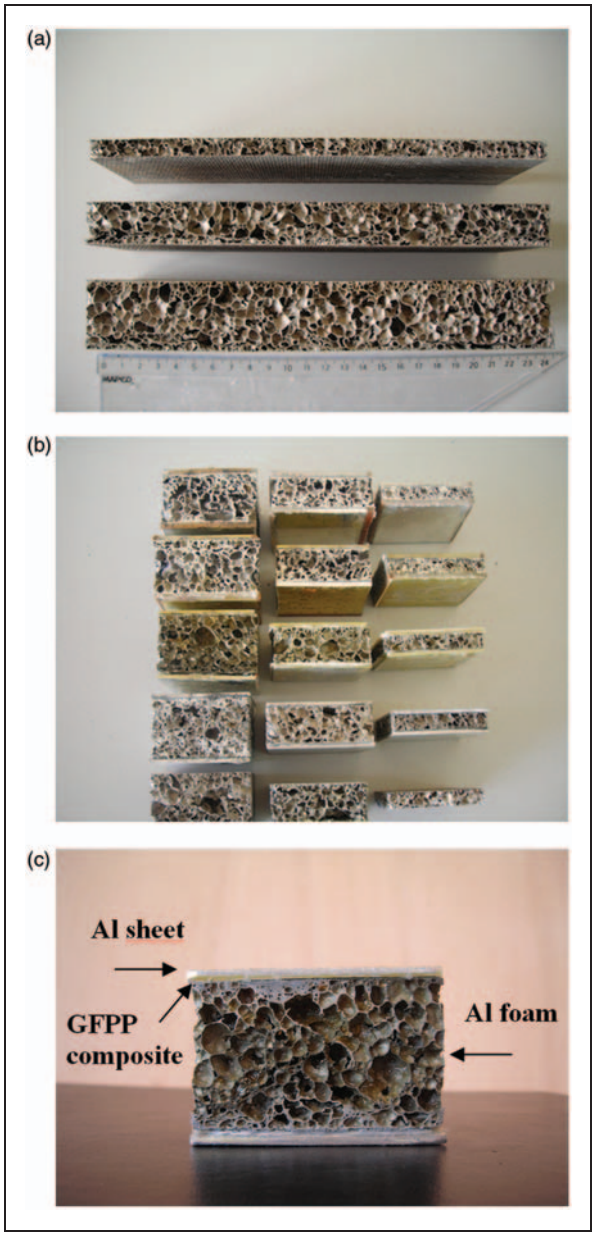

Figure 1. (a) The as-received ALULIGTH™ -AFS Al foam panels with 8, 20, and 30 mm thicknesses. (b) As-received Al foam and AFS made with various foam thicknesses. (c) Al sheet/GFPP/Al foam sandwich structures.

Table 2. Adhesive types and surface modification techniques used for the integration of sandwich components

Sandwich configuration	Adhesive type	Surface modification	Processing technique
Al foam/Al sheet	Epoxy adhesive	–	Cold pressing at room temperature
Al foam/GFPP composite/Al sheet	–	Silane coupling agent	Hot pressing at 200°C and 1.5 MPa
Al foam/GFPP composite/Al sheet	PP adhesive film	–	Hot pressing at 200°C and 1.5 MPa
Al foam/GFPP composite/Al sheet	PP adhesive film	Silane coupling agent	Hot pressing at 200°C and 1.5 MPa

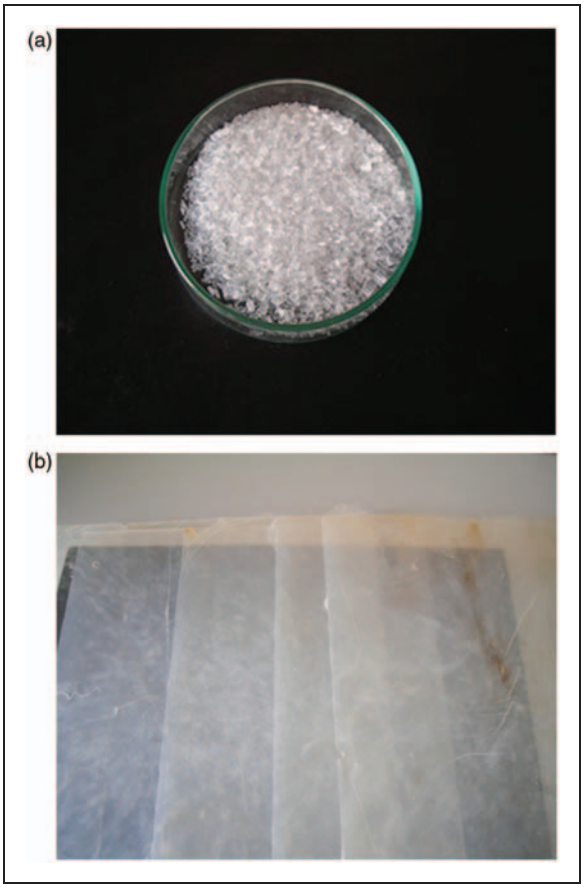

Figure 2. (a) Fine granules of PP-based film and (b) PP-based film containing 20 wt% PP–g–MA produced with extrusion and hot pressing.

sandwiches. The compression test samples were prepared with about $50 \times 50\,mm^2$ by sectioning from larger panels. At least three specimens were tested and force vs. stroke values recorded. All tests were conducted at room temperature using a Schimadzu™ universal test machine at a cross-head speed 2 mm/min. In order to reveal the structures of the sandwiches, the samples were also sectioned and their cross-sections polished. In this study, the macroscopic images of the foam-based structures were taken using a Nikon™ optical microscope.

In this study, both absorbed energy (AE) and specific absorbed energy (SEA) values of the Al foams and

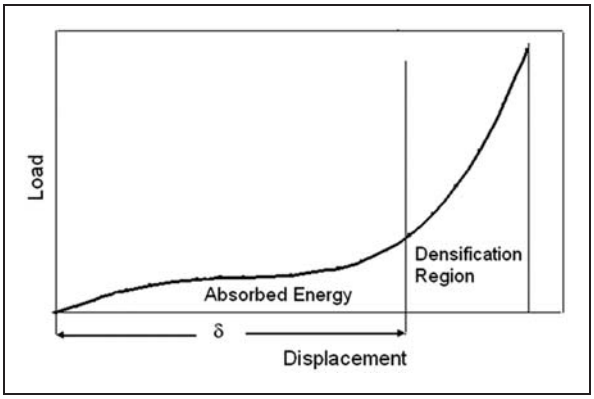

Figure 3. Compression load–displacement curve of ideal foam.

Al foam-based sandwiches were determined. The AEs were calculated from the area under the load–displacement curves of the samples and SAE values were obtained by dividing the energy values by mass. The typical load–displacement graph of compression test is shown in Figure 3, and P, δ, and m parameters used in Equations (1) and (2) represent the load, displacement, and mass of the sandwich, respectively. The elastic modulus (E) is determined from the slope of the elastic part in the stress–strain curve and the collapse stress is defined as the stress at the beginning of the plastic region.

$$\mathrm{AE} = \int_0^{\delta} P\mathrm{d}\delta \tag{1}$$

$$\mathrm{SAE} = \int_0^{\delta} \frac{P\mathrm{d}\delta}{m} \tag{2}$$

Results and discussions

The typical microstructure of an Al foam-based sandwich is given in Figure 4. The 0/90° oriented co-mingled GFPP was placed between Al foam and Al sheet as an intermediate layer. The horizontal lines and small dotted segments in the mid-region are the images of the 0° and 90° oriented fibers, respectively. The foam

Figure 4. Microstructural image of Al sheet/GFPP/Al foam sandwich.

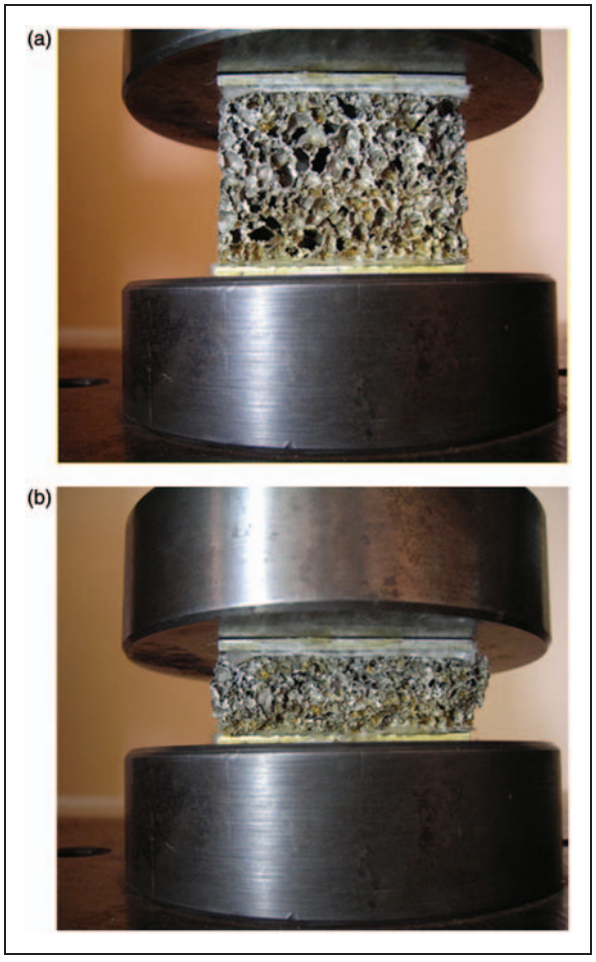

Figure 5. The image of Al sheet/GFPP/Al foam sandwich: (a) before loading and (b) at 50% deformation.

cells are placed under the GFPP composite layer. A typical cell wall image is also seen on the micrograph. The stress–strain behaviors of as-received Al foams and AFS were obtained based on the compression testing. The pictures of a sandwich sample before loading and at 50% deformation are shown in Figure 5(a) and (b), respectively. Figure 6(a)–(e) shows the compressive stress–strain behaviors of as-received Al foams and Al foam-based sandwiches with three different thicknesses under the same loading conditions. At least three specimens per each thickness were tested and typical representative data for each thickness set of specimens are plotted. The deformations were plotted up to 60% strain and the characteristics of the flatwise compression stress–strain curves of sandwich samples showed close similarity with the monolithic Al foams. It is the fact that the densities and the morphological features of the foams showed a close relation with the densification behavior of the samples. It is obvious from Figure 6(a) to (e) that the stress–strain curve initially increases nearly in a linear manner up to a specific value of the compressive stress and then the stress remained almost constant up to a certain value (plateau region). The densification region starts at the completion of the plateau region. The collapse of foam cells ends and they start to densify at a specific strain. As the density of the specimen increases, the plateau region begins to shorten and densification starts at lower strains. Based on the Figure 6(a), the stress values of foams at the same strains vary based on the thickness change. The foams with similar density for each thickness were compared in Figure 6(a) to investigate the mechanical property variation. Although the density difference was smaller than 12%, the 8 mm Al foams showed significantly higher collapse strength and lower elastic modulus. The average elastic modulus and collapse strength values of the Al foams and Al foam-based sandwiches with respect to their densities are given in Table 3. The foam thickness increase resulted in the increase of elastic modulus for the as-received Al foams. It was also revealed from the experimental results that some foams with higher densities showed higher elastic modulus and/or collapse strength values while some of them exhibited the opposite characteristics. A direct correlation was not observed between these parameters due to the variations in foam cell shapes, subsistent defects,

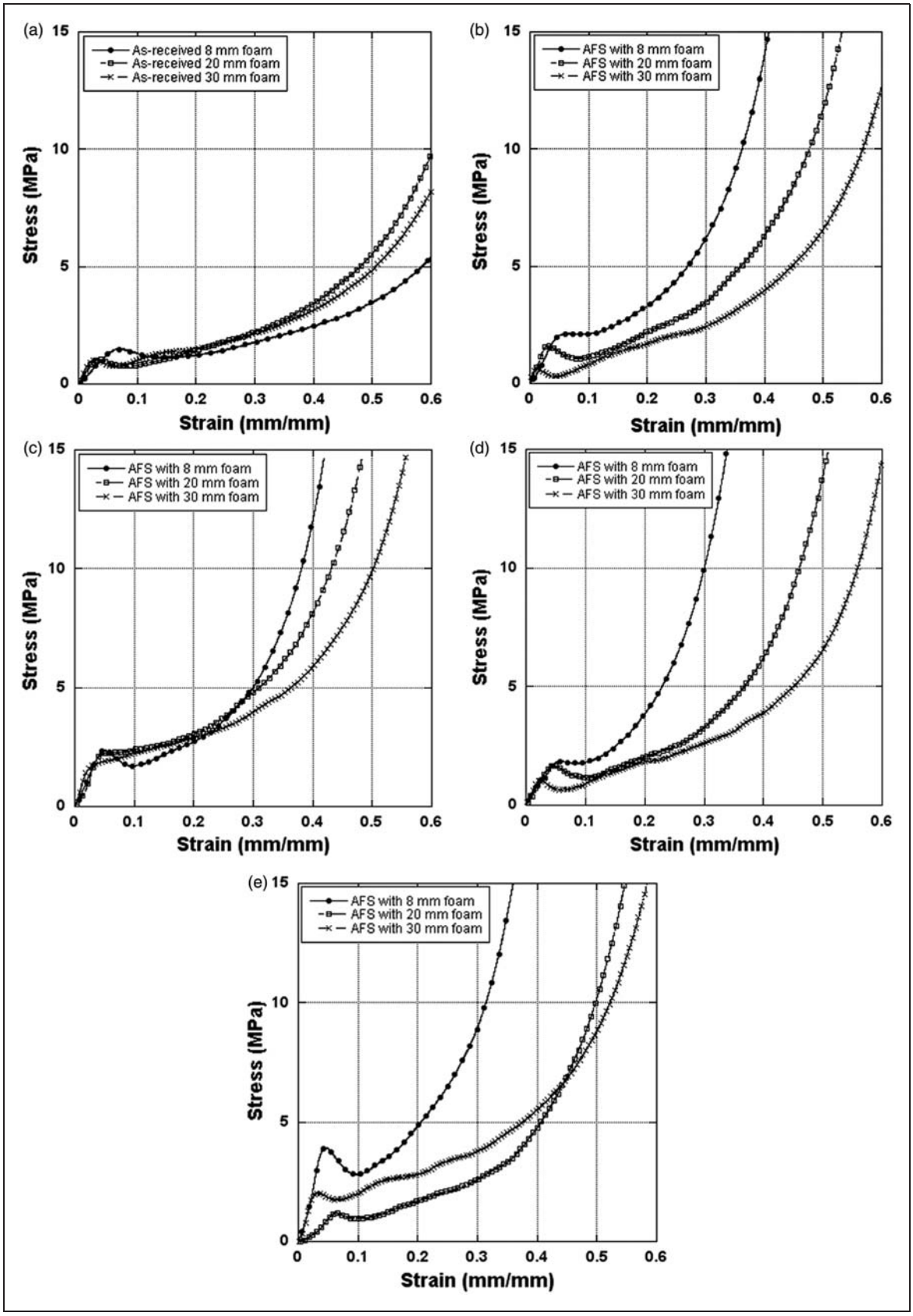

Figure 6. Stress–strain graphs of: (a) as-received Al foams, (b) AFS bonded with epoxy, (c) AFS bonded with GFPP after silane surface treatment, (d) AFS bonded with PP-based film, and (e) AFS bonded with PP-based film after silane surface treatment.

Table 3. Physical and mechanical properties of Al foams and AFS

Sample type (mm)	Average sample density ($g/cm^{3)}$	Average elastic modulus (MPa)	Average collapse strength (MPa)
Al Foam-8	0.33 (0.03)	29.06 (4.78)	2.07 (0.51)
Al Foam-20	0.42 (0.02)	36.21 (4.46)	1.11 (0.08)
Al Foam-30	0.38 (0.06)	54.61 (10.91)	1.15 (0.68)
AFS-8 (epoxy bonded)	1.10 (0.14)	54.45 (11.32)	2.16 (0.82)
AFS-20 (epoxy bonded)	0.80 (0.03)	74.98 (16.27)	1.69 (0.31)
AFS-30 (epoxy bonded)	0.62 (0.02)	58.81 (10.88)	0.66 (0.33)
AFS-8 (silane bonded)	1.14 (0.04)	61.98 (6.39)	2.90 (0.64)
AFS-20 (silane bonded)	0.92 (0.02)	63.71 (10.12)	2.39 (0.57)
AFS-30 (silane bonded)	0.73 (0.07)	77.80 (40.41)	2.05 (0.86)
AFS-8 (PP-based film bonded)	1.14 (0.01)	37.37 (17.92)	1.83 (0.41)
AFS-20 (PP-based film bonded)	0.82 (0.01)	59.10 (33.08)	1.90 (0.92)
AFS-30 (PP-based film bonded)	0.61 (0.04)	47.22 (12.16)	1.03 (0.48)
AFS-8 (silane-treated + PP-based film bonded)	1.16 (0.07)	81.19 (5.63)	3.78 (1.13)
AFS-20 (silane-treated + PP based film bonded)	0.82 (0.04)	42.27 (34.17)	1.31 (0.32)
AFS-30 (silane–treated + PP-based film bonded)	0.66 (0.04)	95.25 (35.26)	2.02 (0.48)

Note: The average values are given with standard deviations.

density, and non-homogeneities of the microstructures. The effects of the foam thickness increase on the behavior of the sandwich structures were also investigated by considering the test results. It was found that the foam thickness increase generally resulted in collapse strength decrease. Also, a significant data scattering was observed, as seen in Table 3. As the thickness increases, the structural defect(s) probably increase(s) and the lower strength values of thicker foams are attributed to this. It was also understood from the experimental results that the foams with higher elastic modulus showed generally higher collapse strength for each thickness set of foam-based sandwiches.

In this study, the SAEs of the Al foams and Al foam-based sandwiches were plotted with respect to strain, as shown in Figure 7(a)–(e). It was found that the foam thickness increase resulted in the increase of AE. Table 4 gives the SAE values of as-received Al foams and Al foam-based sandwiches for various foam thicknesses. The specific energy absorption capacities of the sandwiches were calculated by averaging the SAE values of sandwiches for each thickness set of foam-based sandwiches by considering all bonding types. The sandwiches consisting of 8 mm Al foam completed their densification at 30–60% deformation while the other sandwich samples containing thicker foams reached their highest SAEs at 50–70% strain. In general, the foam thickness increase resulted in the decrease of SAE for both monolithic Al foam and Al foam-based sandwiches at 60% deformation. Based on Table 4, sandwich structures exhibited highest SAE values compared to the as-received foams. This is attributed to the higher densities of sandwich samples which led to the shorter plateau part with higher stresses. The area under the load–displacement curve became larger and thus, both AE values of the sandwiches and SAE parameter increased.

Conclusions

The characterization of aluminum foams and aluminum foam sandwiches were performed by comparing their energy absorption capabilities and mechanical properties such as average elastic modulus and collapse strength values. The samples with higher elastic modulus usually exhibited higher collapse strength for each thickness set of foams and foam-based sandwiches. The foam thickness increase resulted in the increase of elastic modulus for the as-received Al foams and Al foam sandwich systems bonded with GFPP after silane surface treatment. However, the samples bonded with epoxy and integrated with PP-based film with or without surface modification, did not show the same characteristics. The differences among the structures in terms of mechanical properties are attributed to the local density fluctuations and inhomogeneous nature of the aluminum foams. The thickness increase generally leads to the increase of AE and this behavior was also observed in this study. However, the SAE which is the AE per unit mass showed an opposite behavior due to the higher weights of thicker samples. According to the experimental results, the Al sheet/GFPP/Al foam sandwiches showed maximum AE values and this is attributed to contribution of GFPP to the energy

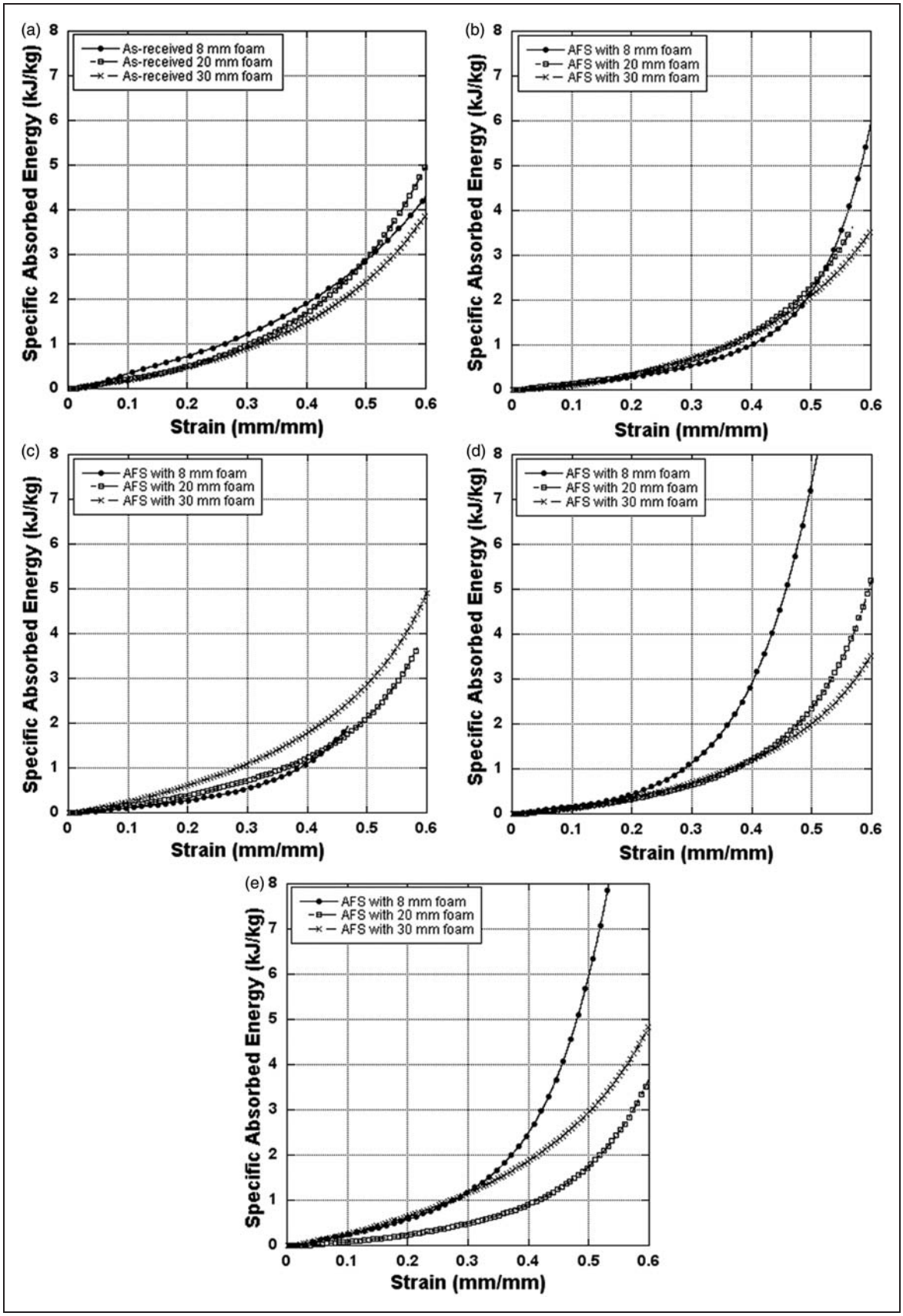

Figure 7. SAE vs. strain graphs of: (a) as-received Al foams, (b) AFS bonded with epoxy, (c) AFS bonded with GFPP after silane surface treatment, (d) AFS bonded with PP-based film, and (e) AFS bonded with PP-based film after silane surface treatment.

Table 4. SAE comparison of as-received Al foams and AFS

Sample type	Foam thickness (mm)	SAE (kj/kg)
As-received Al foam	8	4.48 (0.66)
Al foam based sandwich		6.45 (2.35)
As-received Al foam	20	4.37 (0.56)
Al foam based sandwich		4.39 (0.99)
As-received Al foam	30	3.89 (0.18)
Al foam based sandwich		4.18 (0.83)

Note: The average values are given with standard deviations.

absorption mechanism. In summary, metal/composite sandwiches were fabricated successfully and these structures exhibit high potential for the fabrication of energy absorbing materials with good structural integrity, such as for anti-blast armor or impact-absorbing automotive bumper systems.

Funding

This work was supported by Scientific and Technological Research Council of Turkey (TUBITAK)-107A015 Project.

References

1. Reyes G and Cantwell WJ. The mechanical properties of fiber-metal laminates based on glass fiber reinforced polypropylene. *Compos Sci Technol* 2000; 60: 1085–1094.
2. Langdon GS, Cantwell WJ and Nurick GN. The blast response of novel thermoplastic-based fiber-metal laminates: some preliminary results and observations. *Compos Sci Technol* 2005; 65: 861–872.
3. Ashby MF, Evans AG, Fleck NA, Gibson LJ, Hutchinson JW and Wadley HNG. *Metal foams: A design guide*. Boston, MA, USA: Butterworth-Heinemann Publications, 2000.
4. Giorgi M, Carafalo A, Dattoma V, Nobile R and Palano F. Aluminum foams structural modeling. *Comput Struct* 2009; 88: 25–35.
5. Olurin OB, Fleck NA and Ashby MF. Deformation and fracture of aluminum foams. *Mater Sci Eng A* 2000; 291: 136–146.
6. Idris MI, Vodenitcharova T and Hoffman M. Mechanical behavior and energy absorption of closed cell aluminum foam panels in uniaxial compression. *Mater Sci Eng A* 2000; 517: 37–45.
7. McCullough KYG, Fleck NA and Ashby MF. Uniaxial stress-strain behavior of aluminum alloy foams. *Acta Mater* 1999; 47(8): 2323–2330.
8. Motz C and Pippan R. Deformation behavior of closed-cell aluminum foams in tension. *Acta Mater* 2001; 49: 2463–2470.
9. Deqing W, Weiwei X, Xiangjun M and Ziyuan S. Cell structure and compressive behavior of aluminum foam. *J Mater Sci* 2005; 40: 3475–3480.
10. Koza E, Leonowicza M, Wojciechowski S and Simancik F. Compressive strength of aluminum foams. *Mater Lett* 2003; 58: 132–135.
11. Bastawros AF, Barth-Simith H and Evans AG. Experimental analysis of deformation mechanisms in a closed-cell aluminum alloy foam. *J Mech Phys Solids* 2000; 48: 301–322.
12. Kıratisaevee H and Cantwell WJ. The impact response of aluminum foam sandwich structures based on a glass fiber-reinforced polypropylene fiber-metal laminate. *Polym Compos* 2004; 25: 499–509.
13. McCormack TM, Miller R, Kesler O and Gibson LJ. Failure of sandwich beams with metallic foam cores. *Int J Solids Struct* 2001; 38: 4901–4920.
14. Styles M, Compston P and Kalyanasundaram S. The effect of core thickness on the flexural behavior of aluminum foam sandwich structures. *Compos Struct* 2007; 80: 532–538.
15. Reyes Villanueva G and Cantwell WJ. Low velocity impact response of novel fiber-reinforced aluminum foam sandwich structures. *J Mater Sci Lett* 2003; 22: 417–422.
16. Compston P, Styles M and Kalyanasundaram S. A comparison of low energy impact behavior in aluminum foam and polymer foam sandwich structures. *Sandwich Struct 7: Adv Sandwich Struct Mater* 2003; 22: 643–652.
17. Reyes G. Mechanical behavior of thermoplastic FML-reinforced sandwich panels using aluminum foam core: experiments and modeling. *J Sandwich Struct Mater* 2010; 12: 81–96.
18. Tanoğlu M, Baştürk SB, Merter NE. Mechanical and energy absorption behavior of metal/polymer layered sandwich structures. In: *14th European Conference on Composite Materials, ECCM'10*, Budapest, Hungary, 7–10 June 2010.
19. Dow Corning. Z-6032 silane product information. www.dowcorning.com (2009).